Self-consistent approach to alloys exhibiting partial order*

C. T. White† and E. N. Economou
Department of Physics, University of Virginia, Charlottesville, Virginia 22901
(Received 30 August 1976)

Several self-consistent single-site effective-medium approximations that allow determination within the tight-binding picture of the electronic structure of random binary alloys exhibiting statistical correlation amongst the atomic potentials are presented and developed in detail. The effectiveness of these methods is evaluated by study of the one-dimensional system since there the approximate results can be compared directly to corresponding numerical solutions obtained by solving Schmidt's exact functional equations. As a matter of course extensive results are reported demonstrating the severe effects that correlations can have on the electronic structure of this model alloy. Within the framework of one dimension an n-site cluster approximation is also outlined which is able (by employing clusters made up of as few as five sites) to reproduce accurately the very fine structure of the eigenvalue spectrum. This scheme is applicable to Cayley trees of coordination number other than 2 as well and when coupled with additional approximations will prove useful in investigating localized eigenstates in higher-dimensional systems. Where appropriate these methods are compared both formally and through particular examples to the simple-coherent-potential approximation and also to the cellular-coherent-potential approximation of Butler.

I. INTRODUCTION

In the last several years considerable progress has been made in understanding the electronic structure of disordered systems. Much of the theoretical work involves the use of a tight-binding Hamiltonian formed from atomic orbitals associated with some assumed array of sites. Disorder is usually incorporated into the formalism by taking the site diagonal energies as statistically independent random variables with a given probability distribution. Various approximations are then employed to determine the ensemble-averaged physical quantities of interest. A major development in the theory of such model systems was the coherent-potential approximation (CPA) of Taylor,[1] Soven,[2] and Hubbard.[3] This approximation can be made formally plausible within the multiple-scattering approach of Lax[4] and involves the introduction of an effective medium to be determined self-consistently in such a way that the average electronic scattering from a single "atom" embedded in this medium is zero. Attempts to extend this single-site approximation have occupied many workers.[5-8] One can, for example, entertain the idea of determining the effective medium so that the average scattering from a whole cluster of sites is zero. A notable quantitative success along this line was achieved by Butler[8] within the framework of the standard tight-binding model for a one-dimensional (1D) uncorrelated substitutionally disordered binary alloy. Several extensions of the CPA to tight-binding models with special types of off-diagonal disorder have also been reported.[9] Nevertheless, the theory of disordered models allowed in the tight-binding picture is far from complete.

Here we will study the popular two-level tight-binding model of a substitutionally disordered binary ($A_{X_A}B_{X_B}$) alloy including in the analysis the possibility of statistical correlations amongst the atomic potentials. These atomic correlations (AC) are introduced in the usual way,[10] through a single parameter $P_{A/B}$ representing the probability of finding an A atom at a particular site given a nearest-neighboring site is occupied by a B atom. By varying $P_{A/B}$ from zero to one this model can be made to simulate binary alloys exhibiting a strong tendency towards segregation of species all the way to those having a strong tendency towards compound formation. To date, the vast majority of studies involving the present two-level model have assumed that the atomic potentials are uncorrelated; however, as we shall see, the AC can have severe effects on the electronic structure of this system. Our study of this correlated alloy was originally motivated because of its relationship to a recent apparently highly successful random static one-electron approximation[11] to the Hubbard Hamiltonian. Application of this approximation relies on the existence of computationally rapid and accurate techniques for obtaining the average integrated state density localized about a particular atom (A or B) along with the total integrated density of states (DOS) over the entire range of allowed values of $P_{A/B}$ in the present model. Thus we will focus attention on the development of approximation schemes for determining not only the total DOS (sufficient for a quantitative study of the thermodynamics), but also these conditionally averaged densities of states as well.

The different approximate methods that we will present which allow calculation of these quantities are somewhat similar in spirit to the CPA but are built on the concept of conditional averaging[1,5] which has already been applied by Licciardello and Economou.[12] The first approach we develop is termed the conditional self-consistent approximation (CSA) and is capable of treating our model whenever $P_{A/B} \leq X_A$, while its generalization, the two-sublattice self-consistent approximation (SSA) is applicable for arbitrary $P_{A/B}$. This latter scheme was obtained by coupling to the CSA Licciardello and Economou's idea[12] of employing an effective medium that will reproduce the difficult periodic compound formation limit for equal concentrations of A and B atoms. Unlike the CPA, both the CSA and the SSA are directed toward generating directly the conditionally averaged densities of states from which the total DOS is then determined.

To evaluate the effectiveness of these approximations we have applied them first to the one-dimensional system, since there corresponding exact results can be obtained for comparison by solving Schmidt's functional equations.[10] In this instance we find that both methods are quite successful and particularly accurate for determining the cumulative DOS. Moreover, it is well known that the 1D case provides a severe test[13] for any effective-medium approximation, so that these comparisons provide strong evidence that the CSA and the SSA will be reliable schemes for treating our model in higher dimensions.

In the framework of 1D we have generalized the SSA to an n-site cluster approximation, the cluster SSA (CSSA), which, as we will show, is able to produce accurately the very fine structure known to exist there in the eigenvalue spectrum. It should be noted that in applying this method we have encountered none of the problems such as several possible solutions to the self-consistent equations or negative DOS[7,8,14] that have marred many of the cluster generalizations of the CPA.

The CSSA is applicable to Cayley trees of coordination number other than 2 as well, and when coupled with additional approximations such as those that we will suggest should be very useful in investigating, in particular, localized eigenstates in higher-dimensional lattice structures.

In Sec. II we first describe the model and provide some background leading to our approximation schemes. We then develop the formalism in detail and evaluate the success of the CSA, SSA, and the CSSA by direct comparisons to the exact results in 1D. Additional results showing the effects of AC on Cayley trees of coordination numbers 4 and 6 are also provided. Finally, in Sec. III, we summarize some of the more important features of this work.

II. FORMALISM AND RESULTS

A. Description of the model

We assume that we are dealing with substitutionally disordered binary alloys exhibiting atomic correlations which have an electronic structure that can be adequately described by the one-electron tight-binding Hamiltonain

$$\hat{\mathcal{H}} \equiv \sum_{\vec{n}} |\vec{n}\rangle \epsilon_{\vec{n}} \langle \vec{n}| + \sum_{\vec{l},\vec{m}}{}' |\vec{l}\rangle V_{\vec{l}\vec{m}} \langle \vec{m}| \,, \tag{2.1}$$

where $|\vec{n}\rangle$ represents a Wannier state centered at the site $\vec{n}$ (these sites form some lattice), $V_{\vec{l}\vec{m}}$ is taken as V if $\vec{l},\vec{m}$ are nearest neighbors and zero otherwise, and each $\epsilon_{\vec{n}}$ is a random variable which can assume one of two possible values ϵ^A with probability P_A (equal to the concentration X_A) or ϵ^B with probability $P_B (= 1 - P_A = 1 - X_A)$ depending on whether the site $\vec{n}$ is occupied by an A atom or a B atom, respectively. The possibility of atomic correlations is incorporated into the formalism through four parameters $P_{A/A}$, $P_{A/B}$, $P_{B/A}$, and $P_{B/B}$ where, for example, $P_{A/A}$ represents the probability of finding an A atom at a particular site given a nearest-neighboring site is occupied by an A atom. Due to their definitions, these four quantities are not all independent; in particular we need specify just one, e.g., $P_{A/B}$, to obtain the rest. Note that $P_{A/B}$ satisfies the relation

$$0 \leq P_{A/B} \leq \min[1, X_A/(1 - X_A)] \,, \tag{2.2}$$

with the lower limit corresponding to segregated species and the higher to as close to periodic compound formation as the concentration X_A allows. Since we can choose the zero of energy arbitrarily, the two parameters ϵ^A, ϵ^B can be replaced by a single quantity

$$\delta \equiv (\epsilon^A - \epsilon^B)/V \,, \tag{2.3}$$

which represents the relative scattering strength of the A and B atoms. As mentioned in the Introduction we are interested in developing techniques applicable over the entire space of the parameters $P_{A/B}$, X_A, δ for obtaining the total DOS per site $\rho(E)$ along with the average state densities localized about a particular type of atom, $\rho^\alpha(E)$, $\alpha = A$ or B.

In terms of the model Hamiltonian, the quantities $\rho(E)$ and $\rho^\alpha(E)$ are given by the usual relations:

$$\rho(E) = -(1/\pi)\mathrm{Im} \lim_{s \to 0^+} \langle \mathcal{G}_{\vec{n}\vec{n}}(E + is) \rangle \tag{2.4a}$$

$$\rho^{\alpha}(E) = -(1/\pi)\,\mathrm{Im}\lim_{s\to 0^+}\langle \mathcal{G}_{\vec{n}\vec{n}}(E+is)\rangle_{\vec{n}}^{\alpha}; \quad \alpha = A \text{ or } B, \tag{2.4b}$$

where $\mathcal{G}_{\vec{n}\vec{n}}(Z)$ is the diagonal matrix element of the Green's function $\hat{\mathcal{G}}(Z) \equiv (\hat{Z} - \hat{\mathcal{H}})^{-1}$ with the symbol $\langle\ \rangle$ indicating averaging over all random variables $\{\epsilon_{\vec{l}}\}$ and the symbol $\langle\ \rangle_{\vec{n}}^{\alpha}$ representing an average over the same variables with the exception of $\epsilon_{\vec{n}}$ which is fixed at ϵ^{α}. Obviously,

$$\rho(E) = \sum_{\alpha = A,\,B} X_{\alpha}\rho^{\alpha}(E)\,. \tag{2.5}$$

We will also calculate the average state density localized around a particular compact cluster of atoms $\tilde{c}$ centered at the site $\vec{n}$ which is defined by the number of sites in the cluster and the particular configuration c of A, B atoms over these sites. These quantities will be written for simplicity as $\rho^{c}(E)$ and can be obtained from $\hat{\mathcal{G}}$ through the relation

$$\rho^{c}(E) = -(1/\pi)\,\mathrm{Im}\lim_{s\to 0^+}\langle \mathcal{G}_{\vec{n}\vec{n}}(E+is)\rangle_{\tilde{c}}^{c}\,, \tag{2.6}$$

where $\vec{n}$ is the central site of the cluster and the symbol $\langle\ \rangle_{\tilde{c}}^{c}$ will always represent an average over the random potentials not contained in $\tilde{c}$.

Since our interest lies in calculating the above densities of states, only the diagonal matrix elements of $\hat{\mathcal{G}}$ need to be considered; thus, the approximate schemes developed later will be especially designed to evaluate these quantities. The same techniques, however, can be used to obtain $\langle \mathcal{G}_{\vec{n}\vec{m}}\rangle_{\tilde{c}}^{c}$ when either $\vec{m}$ belongs to $\tilde{c}$ or the distance $|\vec{n} - \vec{m}|$ is less than a characteristic length associated with the correlation implied by the difference $|P_{A/B} - X_A|$. For larger $|\vec{n} - \vec{m}|$ our methods are not directly applicable, but can be used indirectly by first expressing $\mathcal{G}_{\vec{n}\vec{m}}$ as a function of diagonal matrix elements, then calculating the average of the latter, and finally assuming that the average $\mathcal{G}_{\vec{n}\vec{m}}$ is given by the same function in terms of the average diagonal matrix elements. The errors that the last assumption may introduce are probably as severe as the ones present in the simple CPA. Thus we consider our approximation accurate and therefore applicable for calculating diagonal matrix elements $\langle \mathcal{G}_{\vec{n}\vec{n}}\rangle_{\tilde{c}}^{c}$ and off-diagonal matrix elements $\langle \mathcal{G}_{\vec{n}\vec{m}}\rangle_{\tilde{c}}^{c}$ when $|\vec{n} - \vec{m}|$ is less than a characteristic distance depending on $\tilde{c}$ and $|P_{A/B} - X_A|$. Here we will report results only for diagonal matrix elements.

B. Basic ideas; notation

The approximation schemes that we will employ here are directed toward determining the conditionally averaged Green's functions from which the totally averaged quantities can be obtained. Thus $\langle \mathcal{G}_{\vec{n}\vec{n}}\rangle$ will be calculated by first expressing it as

$$\langle \mathcal{G}_{\vec{n}\vec{n}}\rangle = \sum_{c} P(c)\langle \mathcal{G}_{\vec{n}\vec{n}}\rangle_{\tilde{c}}^{c}\,, \tag{2.7}$$

where $P(c)$ represents the probability of a particular configuration c of the A, B atoms over a cluster $\tilde{c}$, and then approximating each $\langle \mathcal{G}_{\vec{n}\vec{n}}\rangle_{\tilde{c}}^{c}$ separately.

To find $\langle \mathcal{G}_{\vec{n}\vec{n}}\rangle_{\tilde{c}}^{c}$ we first introduce the effective hybrid Hamiltonian

$$\hat{H}^{c} \equiv \sum_{\vec{m}\in\tilde{c}} |\vec{m})\,\epsilon_{\vec{m}}(\vec{m}| + \sum_{\vec{m}\notin\tilde{c}} |\vec{m})\sigma_{\vec{m}}^{c}(\vec{m}| + \sum_{\vec{l},\,\vec{m}}{}' |\vec{l})\,V_{\vec{l}\vec{m}}(\vec{m}|\,, \tag{2.8}$$

which is obtained from $\hat{\mathcal{H}}$ by replacing all $\epsilon_{\vec{m}}$ for $\vec{m}$ not belonging to the cluster $\tilde{c}$ by the nonrandom (but yet unspecified) coherent potentials $\{\sigma_{\vec{m}}^{c}\}$. We then take

$$\langle \mathcal{G}_{\vec{n}\vec{n}}\rangle_{\tilde{c}}^{c} \approx (\vec{n}|\,(\hat{Z} - \hat{H}^{c})^{-1}\,|\vec{n}) = G_{\vec{n}\vec{n}}^{c}\,, \tag{2.9}$$

with the quantities $\{\sigma_{\vec{m}}^{c}\}$ being determined in such a way that Eq. (2.9) is satisfied as accurately as is practical. From the definition of Green's function, it follows that

$$\hat{\mathcal{G}} = \hat{G}^{c} + \hat{G}^{c}\hat{T}^{c}\hat{G}^{c}\,, \tag{2.10}$$

where $\hat{T}^{c}$ is the usual scattering matrix defined through the relations $\hat{T}^{c} = (\hat{1} - \hat{V}^{c}\hat{G}^{c})^{-1}\hat{V}^{c}$, $\hat{V}^{c} = \hat{\mathcal{H}} - \hat{H}^{c}$. Thus (2.9) would be exact if $\{\sigma_{\vec{m}}^{c}\}$ could be chosen so that

$$\langle \hat{T}^{c}\rangle_{\tilde{c}}^{c} = 0\,. \tag{2.11}$$

Now following a similar line of thought that led to the simple CPA, we replace (2.11) by

$$\langle \hat{t}_{\vec{m}}^{c}\rangle_{\tilde{c}}^{c} = 0\,, \quad \vec{m}\notin\tilde{c} \tag{2.12}$$

where $\hat{t}_{\vec{m}}^{c}$ is the t matrix associated with the scattering potential $|\vec{m})(\epsilon_{\vec{m}} - \sigma_{\vec{m}}^{c})(\vec{m}|$ and the unperturbed Hamiltonian $\hat{H}^{c}$. The conditional average in (2.12) is only over the single random variable $\epsilon_{\vec{m}}$, since this is the only such quantity entering $\hat{t}_{\vec{m}}^{c}$. Note that one could generalize (2.12) by replacing the sites $\{\vec{m}\}$ by appropriate clusters of sites outside the basic cluster $\tilde{c}$. In the present work, however, we will not consider such extensions and will rather use throughout equations of the form (2.12) to determine the coherent potentials $\sigma_{\vec{m}}^{c}$. Obviously from a calculational point of view one can use only a small number of different $\sigma_{\vec{m}}^{c}$ which must be arranged over the sites $\{\vec{m}\}$ $(\vec{m}\notin\tilde{c})$ in a systematic way so that $\hat{G}^{c}$ can be determined explicitly. However, in doing so (2.12) can no longer be satisfied at all sites $\vec{m}$ and thus one has to decide

at which sites it will be maintained.

The approximation scheme outlined above can be characterized by: (i) size, shape, and position of the cluster $\bar{c}$; clearly $\bar{c}$ should contain $\vec{n}$ so as to reproduce the atomic limit ($V=0$). In addition, the larger and more symmetric (about $\vec{n}$) the cluster, the better the approximation. This can be seen from Eq. (2.10) which implies that the correction to approximation (2.9) has a factor of the form $G^c_{\vec{n}\vec{m}}G^c_{\vec{m}\vec{m}}$ with $|\vec{n}-\vec{m}|$ larger than the radius of the cluster [because by definition $(\vec{k}|\hat{T}^c|\vec{k}')=0$ for $\vec{k},\vec{k}'\in\bar{c}$]. However, $G^c_{\vec{n}\vec{m}}=0$ when $V=0$ and is also known to decrease rather rapidly with increasing $|\vec{n}-\vec{m}|$. A more physical way of putting all of this is to simply say that $\mathcal{G}_{\vec{n}\vec{m}}$ depends mostly on the immediate environment of $\vec{n}$ which is reproduced exactly within the cluster $\bar{c}$. On the other hand, the larger the cluster $\bar{c}$, the more complicated the calculation becomes. (ii) The number of independent coherent potentials $\sigma^c_{\vec{m}}$ and their distribution among the sites $\vec{m}$, where $\vec{m}\in\bar{c}$; as a general tendency the more σ's available, the more accurate the scheme can be made. On the other hand, the choice of σ's should be such that certain symmetry requirements can be satisfied and the quantities $G^c_{\vec{n}\vec{m}}$ can be obtained. (iii) The position of the sites $\vec{m}$ outside the cluster $\bar{c}$ where Eq. (2.12) is to be satisfied; one has to choose as many sites as the number of self-consistently determined σ's in order to have as many equations as unknowns. Also by varying the location of these sites the resultant approximation can be made better or worse. By making different choices in the above three aspects of the present approximation technique, one can generate a host of various specific approximation schemes. Below we examine three such schemes starting with the simplest.

C. Conditional self-consistent approximation (CSA)

In this approximation the cluster $\bar{c}$ is taken as consisting of the central atom $\vec{n}$ only; further, all the coherent potentials $\sigma^\alpha_{\vec{m}}$ are considered equal. Thus the effective hybrid medium is as in Fig. 1(b) (for the 1D case). It remains to choose the site $\vec{m}$ at which the basic equation (2.12) will be satisfied. Here $\vec{m}$ is chosen as a nearest-neighboring site to $\vec{n}$. One can argue in favor of this location of $\vec{m}$ by noting that the potentials on sites closer to $\vec{n}$ have more important effects on $\langle\mathcal{G}_{\vec{n}\vec{n}'}\rangle^\alpha_{\vec{n}}$ than those associated with more distant sites. Also, by symmetry if Eq. (2.12) is satisfied at one nearest neighbor of $\vec{n}$, it is satisfied at all other nearest-neighboring sites as well.

The CSA thus obtains $\langle\mathcal{G}_{\vec{n}\vec{n}'}\rangle$ through Eq. (2.7) by taking each

$$\langle\mathcal{G}_{\vec{n}\vec{n}'}\rangle^\alpha_{\vec{n}}\approx G^\alpha_{\vec{n}\vec{n}'};\quad \alpha=A \text{ or } B, \tag{2.13}$$

where

$$\hat{G}^\alpha=(\hat{Z}-\hat{H}^\alpha)^{-1}, \tag{2.14}$$

and

$$\hat{H}^\alpha=|\vec{n})\epsilon^\alpha(\vec{n}|+\sum_{\vec{m}\neq\vec{n}}|\vec{m})\sigma^\alpha(\vec{m}|+\sum_{\vec{l}\vec{l}'}{}'|\vec{l})V_{\vec{l}\vec{l}'}(\vec{r}|\,. \tag{2.15}$$

The quantity σ^α is determined from the condition

$$\langle\hat{t}^\alpha_{\vec{m}}\rangle^\alpha_{\vec{n}}=0, \tag{2.16}$$

where the site $\vec{m}$ is a nearest neighbor of $\vec{n}$,

$$\hat{t}^\alpha_{\vec{m}}=|\vec{m})\frac{\epsilon_{\vec{m}}-\sigma^\alpha}{1-(\epsilon_{\vec{m}}-\sigma^\alpha)G^\alpha_{\vec{m}\vec{m}}}(\vec{m}|\,, \tag{2.17}$$

and $G^\alpha_{\vec{m}\vec{m}}$ can be easily determined since it corresponds to a periodic Hamiltonian with one impurity at the site $\vec{n}$. The CSA is schematically outlined (for the 1D chain) from a slightly different point of view in Fig. 1.

The coherent potentials σ^A,σ^B can be complex and different and are of course independent. Note, the effective potential σ^A is totally determined by employing techniques discussed in the Appendix to solve the single equation (2.16) with $\alpha=A$ and in a similar fashion σ^B is obtained by solving this equation with $\alpha=B$. Thus to approximate $\langle\mathcal{G}_{\vec{n}\vec{n}'}\rangle^A_{\vec{n}}$, the CSA employs an effective medium characterized by σ^A, while to approximate $\langle\mathcal{G}_{\vec{n}\vec{n}'}\rangle^B_{\vec{n}}$, it employs a different effective medium characterized by σ^B. It may seem that it is a rather severe approximation to allow the effects of conditional averaging (i.e., fixing the random variable $\epsilon_{\vec{n}}$ at either ϵ^A or ϵ^B) to be reflected in the reference medium all the way to infinite distance from $\vec{n}$. However, the benefits realized by making the medium, to be

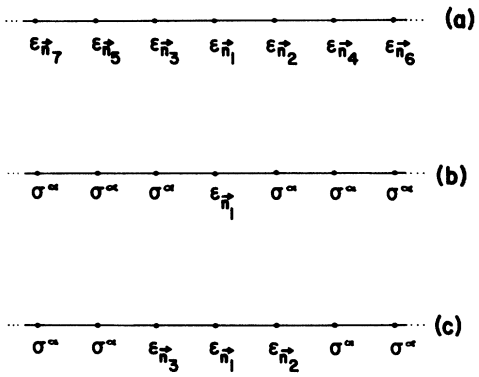

FIG. 1. Schematic outline of the CSA which first replaces the actual random medium (a) by the hybrid random medium (b) and then determines the free nonrandom parameter σ^α in such a way as to make (b) behave as much like (c) as possible insofar as the quantity $\langle\mathcal{G}_{\vec{n}\vec{n}}\rangle^\alpha_{\vec{n}}$ is concerned.

used in obtaining the approximation for $\langle \mathcal{G}_{\vec{n}\vec{n}} \rangle^B_{\vec{n}}$ ($\langle \mathcal{G}_{\vec{n}\vec{n}} \rangle^A_{\vec{n}}$), locally aware, as it should be, that the site $\vec{n}$ is occupied by a B (an A) atom, will turn out to outweigh the mistakes made by forcing this awareness to large distances from $\vec{n}$. As a matter of fact, as we shall see, the CPA makes just the opposite and usually more severe mistake in self-consistently defining its effective medium.

Regardless of whether $\alpha = A$ or B, Eq. (2.16) will have several solutions, each of which is a function of Z. Always the correct solution is chosen by its asymptotic behavior as $|Z|$ approaches infinity, and then followed numerically to the interesting range of energies within the band. We emphasize that in all instances when we have applied the CSA to systems partially characterized by large δ, no problems were encountered in using this procedure to obtain the approximate density of states over the entire band. This is in marked contrast to several other effective-medium theories that suffer great difficulties in continuing the correct solutions from infinity when treating systems with large δ, due to the appearance of physically inadmissible nonanalyticities in their respective effective Green's function.[7,8,14]

That the CSA's way of defining the $\{\sigma^\alpha_{\vec{m}} | \vec{m} \neq \vec{n}\}$ will produce the correct results for $\langle \mathcal{G}_{\vec{n}\vec{n}} \rangle$ in the uncorrelated periodic limits of the model follows easily, since Eq. (2.16) clearly requires in any of these limits that σ^α be equal to $\langle \epsilon_{\vec{m}} \rangle^\alpha_{\vec{n}}$, where $\vec{m}$ is the nearest neighbor of $\vec{n}$; a result which will yield $\sigma^\alpha = \bar{\epsilon} \equiv X_A \epsilon^A + X_B \epsilon^B$ when coupled with the assumed statistical independence of the site-diagonal energies. Further, the CSA will reproduce the correct results to first order around these limits as well.

To demonstrate this last point we can recast, the defining Eq. (2.16) for σ^α into the form

$$\bar{\epsilon} - \sigma^\alpha - (\epsilon^B - \sigma^\alpha) G^\alpha_{\vec{m}\vec{m}} (\epsilon^A - \sigma^\alpha) = 0 , \tag{2.18}$$

which allows us to see that when $|\delta| = |\epsilon^A - \epsilon^B|/V \ll 1$ we have $\sigma^\alpha = \bar{\epsilon}$ to first order in δ. Thus, our approximate expression for $\langle \hat{\mathcal{G}} \rangle$ is simply the virtual crystal propagator which is trivially correct to $O(\delta)$ in this weak scattering uncorrelated limit. To investigate the limits of vanishing concentration of either species we first for definiteness suppose $X_A = 1 - \eta, X_B = \eta$, where $\eta \ll 1$, and then partially solve Eq. (2.18) to obtain

$$\sigma^\alpha = \epsilon^A + \frac{(\epsilon^B - \epsilon^A)\eta}{1 - (\epsilon^B - \sigma^\alpha) G^\alpha_{\vec{m}\vec{m}}} . \tag{2.19}$$

Iterating this result, we have immediately to $O(\eta)$ that

$$\sigma^\alpha = \epsilon^A + (\epsilon^B - \epsilon^A)\eta / [1 - (\epsilon^B - \epsilon^A) G^\alpha_{\vec{m}\vec{m}}] . \tag{2.20}$$

By putting these values of σ^A, σ^B back into their respective hybrid Hamiltonians and using the fact that

$$\langle \hat{\mathcal{G}} \rangle = \sum_{\alpha = A, B} X_\alpha \hat{G}^\alpha_{\vec{n}\vec{n}} \tag{2.21}$$

we find, by only retaining terms of $O(\eta)$, that

$$\langle \hat{\mathcal{G}} \rangle = \hat{R}^A + \frac{(\epsilon^B - \epsilon^A)\eta}{1 - (\epsilon^B - \epsilon^A)\hat{R}^A_{\vec{n}\vec{n}}} \sum_{\vec{k}} \hat{R}^A |\vec{k}\rangle\langle\vec{k}| \hat{R}^A , \tag{2.22}$$

where $\hat{R}^A \equiv (\hat{Z} - \hat{K}^A)^{-1}$ and $\hat{K}^A$ is the tight-binding Hamiltonian for a perfect A crystal. This propagator is just what one would obtain by solving the problem of ηN (N is the total number of sites in the lattice) independent B impurities in a host A lattice and as such is correct to $O(\eta)$.

In order to further investigate what kind of errors are introduced by the CSA one can use standard techniques[15] to express $\langle \hat{\mathcal{G}} \rangle^\alpha_{\vec{n}}$ in powers of $\hat{G}^\alpha$ and $\hat{t}^\alpha_{\vec{m}}$, $\vec{m} \neq \vec{n}$; doing this allows one to see that in the absence of correlation ($P_{A/B} = X_A$), the lowest-order corrections to the CSA from sites close to $\vec{n}$ are of the form

$$(\vec{n} | \hat{G}^\alpha \hat{t}^\alpha_{\vec{m}} \hat{G}^\alpha \hat{t}^\alpha_{\vec{k}} \hat{G}^\alpha \hat{t}^\alpha_{\vec{m}} \hat{G}^\alpha \hat{t}^\alpha_{\vec{k}} \hat{G}^\alpha | \vec{n}) ,$$

i.e., fourth order in t, where $\vec{m}, \vec{k}$ are two different nearest neighbors of $\vec{n}$. Thus the vicinity of $\vec{n}$ is treated rather accurately in the CSA.

The CSA can be brought into immediate contact with the familiar CPA in the regime where the latter approach is applicable ($P_{A/B} = X_A$) by first recalling that the CSA was obtained by choosing the site $\vec{m}$ at which Eq. (2.16) is satisfied to be as close as possible to the central site $\vec{n}$, and then noting that if we had chosen instead the opposite limiting case of taking $\vec{m}$ at infinite distance from $\vec{n}$, we would have recovered the simple CPA. This follows since

$$\langle \hat{t}^\alpha_{\vec{m}} \rangle^\alpha_{\vec{n}} \overset{P_{A/B} = X_A}{=} \langle \hat{t}^\alpha_{\vec{m}} \rangle \to \langle \hat{t}_{\vec{m}} \rangle \text{ as } |\vec{n} - \vec{m}| \to \infty$$

and hence Eq. (2.16) reduces to the basic CPA equation $\langle \hat{t}_{\vec{m}} \rangle = 0$. This clarifies the similarities as well as the differences between the two approaches. More explicitly, the CSA chooses a site as close as possible to $\vec{n}$ to partially incorporate the effects that arise from fluctuations of the actual medium around the reference medium in the immediate vicinity of $\vec{n}$. However, to achieve this it uses an effective medium that incorrectly reflects all the way to infinite distance from $\vec{n}$ the effect of fixing the random variable $\epsilon_{\vec{n}}$ at ϵ^α. On the other hand, the CPA in taking $\vec{m}$ an infinite distance from $\vec{n}$ defines an effective medium that is correct insofar as it does not reflect at infinity the fixing of $\epsilon_{\vec{n}}$ at ϵ^α, but to achieve this, it gives up a lot to the CSA by extending this medium incorrectly into the neighborhood of the fixed site. The two methods thus make complementary

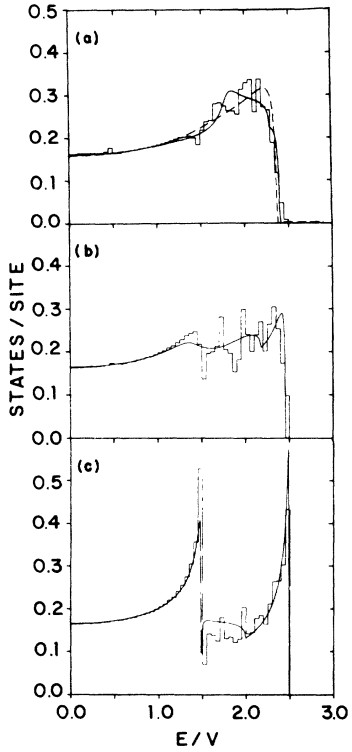

FIG. 2. Total density of states obtained by employing the CSA (solid lines) and where applicable, the CPA (dashed line) compared with the exact density of states (histogram) for a 1D disordered alloy with $X_A = X_B = 0.5$, $\delta = 1$, and (a) $P_{A/B} = 0.5$, (b) $P_{A/B} = 0.3$, and (c) $P_{A/B} = 0.1$. If the CPA were applied to cases (b) and (c), it would yield the same results as in case (a). All curves are symmetric about: $(\epsilon^A + \epsilon^B)/V \equiv 0$.

mistakes. In particular, right around the limits $X_A = 0$ or 1; $\delta = 0$, the CPA is the better approximation since in these limits the effects of fixing $\epsilon_{\vec{n}}$ should be minimal and thus "much" overstressed by the CSA; however, whenever the electron's mean free path is short, but not zero, the CSA is expected to be the better approximation since the effects on $\langle \mathcal{G}_{\vec{n}\vec{m}} \rangle^{\alpha}_{\vec{n}}$ due to the environment in the immediate vicinity of $\vec{n}$, stressed by this scheme but ignored entirely by the CPA, should play the more important role. The price paid to the CPA by the CSA around the coherent limits of the model when $X_A = P_{A/B}$ as far as approximating the totally averaged DOS is concerned is actually small since, as we have shown, the CSA reproduces around these limits the correct Green's function at least to first order. Furthermore, in the more interesting uncorrelated cases where $|\delta|$ is becoming fairly large and the concentration of both constituents appreciable, it turns out that the CSA more than recoups any debt incurred to the CPA in the neighborhood of $\delta \to 0$ or $X_\alpha \to 0$ since here comparison of the approximate CSA and CPA densities of states to corresponding results obtained by solving Schmidt's exact equation show a systematic and substantial superiority in the CSA's results. More specifically, as δ is increased, the CSA is progressively better than the CPA in producing the band edges, cumulative total density of states, and some of the erratic structure of the band. This phenomenon is easily understood in the light of our above analysis since as the relative scattering strength is increased, the mean free path of the electron should decrease, thus making the CSA increasingly better than the CPA. As can be seen from Fig. 2, in 1D, when $X_A = X_B$, the CSA is already actually the more satisfactory approach for values of δ as low as one. This is perhaps somewhat surprising since in this example the total DOS is not that different from what would be obtained from the virtual-crystal approximation. We emphasize, however, that these results are from 1D where the effects of the local environment on the total DOS are usually more important.

Up to this point we have only examined some of the ramifications of applying the CSA to uncorrelated alloys ($X_A = P_{A/B}$). However, this approach in contrast to the CPA has the ability to incorporate effects on the state densities of interest associated with a tendency of the A, B atoms to segregate. More specifically, the effective medium that we employ in the CSA to approximate $\langle \mathcal{G}_{\vec{n}\vec{m}} \rangle^{\alpha}_{\vec{n}}$ will quite naturally treat some of the effects of taking $P_{A/B} \leq X_A$, and in particular, will allow the reproduction of the limit $P_{A/B} \to 0$. That the CSA yields the correct results when $P_{A/B} = 0$ follows by first noting that here $P_{A/A} = P_{B/B} = 1$ and $P_{A/B} = P_{B/A} = 0$ regardless of the value of X_A so that Eq. (2.16) can be trivially solved to find that

$$\sigma^{\alpha} = \langle \epsilon_{\vec{m}} \rangle^{\alpha}_{\vec{n}} = \begin{cases} \epsilon^A & \text{if } \alpha = A \qquad (2.23a) \\ \epsilon^B & \text{if } \alpha = B\,. \qquad (2.23b) \end{cases}$$

Thus, when $P_{A/B} = 0$, the CSA in calculating $\langle \mathcal{G}_{\vec{n}\vec{n}} \rangle^{A}_{\vec{n}}$ ($\langle \mathcal{G}_{\vec{n}\vec{n}} \rangle^{B}_{\vec{n}}$) replaces this quantity with the diagonal matrix element of the Green's function for a perfect A (B) crystal having the same lattice structure as the disordered system, which is just the correct result. A correlated random binary alloy with $P_{A/B}$ finite, but a lot less than X_A can be simply interpreted as a system composed of very large domains of all A or B atoms on the microscopic scale which are still small however on the macroscopic scale. An obvious analogy exists here with Weiss's explanation in terms of ferromagnetic domains of the experimental fact that the total magnetic moment of a ferromagnet can be very much less than the saturation moment at temperatures well below the Curie point.

Since the CSA reproduces the limit $P_{A/B}=0$ and works quite well when $X_A=P_{A/B}$ it provides an interpolation scheme throughout the regime $P_{A/B} \leq X_A$. To analyze somewhat whether this is a reasonable interpolation scheme we first note that if we apply the CSA to an alloy with $P_{A/B}<X_A$, we make a sacrifice in this approximation's ability to precisely incorporate many of the more important average effects on the quantities of interest that arise from local fluctuations of the random medium around the reference medium at nearest-neighboring sites to where $\langle \mathcal{G}_{\vec{n}\vec{n}} \rangle_{\vec{n}}^{\alpha}$ is to be calculated. For example, there are now correction terms (associated with nearest neighboring sites of $\vec{n}$) to the CSA that are second order in t and not fourth order as in the uncorrelated case since now all the random scattering vertices $\hat{t}_{\vec{m}}^{\alpha}$ become statistically dependent. In this sense, the CSA could be expected to progressively worsen as an approximation to $\langle \mathcal{G}_{\vec{n}\vec{n}} \rangle_{\vec{n}}^{\alpha}$ as $P_{A/B}$ becomes more and more different from X_A; however, as $P_{A/B}$ decreases from its uncorrelated value, the present approach could also be expected to improve due to a systematic reduction in the magnitude of the average fluctuations of the random medium around the self-consistent reference medium in the neighborhood of a site known to be occupied by an atom of a given type. This follows of course because of the tendency of the system to form large clusters locally of one type of the atom and it is just through this process that the CSA recovers the limit $P_{A/B} \to 0$. Since the CSA employs this type of balancing, it can be expected to work fairly well in the regime $P_{A/B} \leq X_A$. These expectations are in fact realized for the 1D cases where we have compared results obtained by applying this approximation to corresponding results generated by solving Schmidt's function equations. Some examples are shown in Figs. 2(b) and 2(c). In light of these and other results (not shown) in 1D, we can make a strong conjecture to the effect that the CSA will prove a surprisingly accurate technique for obtaining both the conditionally and totally averaged densities of states in our model when $P_{A/B} \leq X_A$ regardless of the dimensionality of the system, since in higher dimensions the effects on the quantities we wish to approximate of the more important fluctuations neglected by the CSA are expected to lessen rather than to increase. Thus the CSA is expected to be very useful in analyzing both quantitatively and qualitatively the effects on the electronic structure of random alloys due to a tendency toward segregation of species ($P_{A/B} \leq X_A$) in real higher-dimensional systems.

When $X_A=0.5$, the CSA is of course unable to effectively approximate $\langle \mathcal{G}_{\vec{n}\vec{n}} \rangle_{\vec{n}}^{\alpha}$ as $P_{A/B}$ approaches one due to its inability to reflect the increase at this limit of the number of atoms per unit cell. For this reason, we have developed the SSA described below which is capable of reproducing this difficult periodic compound formation limit along with the other coherent limits of the model and represents in almost all instances an improvement over the CSA.

D. Two-sublattice self-consistent approximation (SSA)

In this approximation, as in the CSA, the cluster $\tilde{c}$ is chosen in the simplest possible way as consisting of the site $\vec{n}$ only. In choosing the number and the arrangement of the coherent potentials $\sigma_{\vec{m}}^{c}$, $\vec{m} \neq \vec{n}$, we first note that when $X_A=0.5$ and $P_{A/B}=1$, the system divides into two interpenetrating sublattices which have no sites in common, with the sites of one sublattice being occupied only by A atoms and the sites of the other only by B atoms. Under these circumstances, if we separate the self-consistent equations (2.12) into two groups, with one group being associated with sites of one sublattice and the other group associated with sites of the other sublattice, then in the limit $X_A \to 0.5$, $P_{A/B} \to 1$, all the equations in a particular group have the same physically correct solutions. Thus if we, when approximating $\langle \mathcal{G}_{\vec{n}\vec{n}} \rangle_{\vec{n}}^{\alpha}$ by $G_{\vec{n}\vec{n}}^{\alpha}$, define the reference medium as composed of two sublattices each characterized by a single coherent potential and determine these two potentials self-consistently by requiring that $\langle \hat{t}_{\vec{m}}^{\alpha} \rangle_{\vec{n}}^{\alpha}=0$, $\langle \hat{t}_{\vec{r}}^{\alpha} \rangle_{\vec{n}}^{\alpha}=0$, where $\vec{r}, \vec{m}$ are sites in different sublattices, we have generated an approximation scheme which reproduces the limit $X_A \to 0.5$, $P_{A/B} \to 1$. It should be clear from our previous discussion that this way of determining $\{\sigma_{\vec{m}}^{\alpha}\}$ will incorporate the other coherent limits of the model as well. In the spirit of the CSA, we now choose $\vec{m}, \vec{r}$ to be as close as possible to $\vec{n}$ so as to include on the average in the approximate Green's function a partial description of the local environment around the site $\vec{n}$ which is expected to have the most important determining effects on the state densities when the mean free path of the electron is short. With these specifications, the SSA is now defined and can be summarized as obtaining

$$\rho^{\alpha}(E) = -(1/\pi)\,\mathrm{Im} \lim_{s \to 0^{+}} \langle \mathcal{G}_{\vec{n}\vec{n}}(E+is) \rangle_{\vec{n}}^{\alpha}; \quad \alpha = A \text{ or } B, \tag{2.24}$$

approximately by taking

$$\langle \hat{\mathcal{G}} \rangle_{\vec{n}}^{\alpha} \approx G^{\alpha} = (\hat{Z} - \hat{H}^{\alpha})^{-1}, \tag{2.25}$$

where here the hybrid Hamiltonian $\hat{H}^{\alpha}$ takes the explicit form

$$\hat{H}^{\alpha} \overset{\text{SSA}}{=} |\vec{n}) \epsilon^{\alpha}(\vec{n}| + \sum_{\vec{m} \in S_1} |\vec{m}) \sigma_1^{\alpha}(\vec{m}| + \sum_{\vec{r} \in S_2} |\vec{r}) \sigma_2^{\alpha}(\vec{r}| + \sum_{\vec{l},\vec{m}}{}' |\vec{l}) V(\vec{m}|, \tag{2.26}$$

with S_2 representing the sublattice which contains $\vec{n}$, S_1 the other sublattice, and with the quantities $\sigma_1^\alpha, \sigma_2^\alpha$ being determined through the relations

$$\langle \hat{t}^{\alpha}_{\vec{m}} \rangle^{\alpha}_{\vec{n}} = 0; \quad \langle \hat{t}^{\alpha}_{\vec{r}} \rangle^{\alpha}_{\vec{n}} = 0 , \tag{2.27}$$

where $\vec{m}$ and $\vec{r}$ are nearest- and next-nearest-neighboring sites, respectively, to $\vec{n}$.

For the purposes of numerical calculations Eqs. (2.27) can be recast in the more convenient form

$$\bar{\epsilon}_1^\alpha - \sigma_1^\alpha - (\epsilon^B - \sigma_1^\alpha) G^{\alpha}_{\vec{m}\vec{m}} (\epsilon^A - \sigma_1^\alpha) = 0 , \tag{2.28a}$$

$$\bar{\epsilon}_2^\alpha - \sigma_2^\alpha - (\epsilon^B - \sigma_2^\alpha) G^{\alpha}_{\vec{r}\vec{r}} (\epsilon^A - \sigma_2^\alpha) = 0 , \tag{2.28b}$$

where $\bar{\epsilon}_1^\alpha \equiv \langle \epsilon_{\vec{m}} \rangle^{\alpha}_{\vec{n}}$, $\bar{\epsilon}_1^\alpha \equiv \langle \epsilon_{\vec{r}} \rangle^{\alpha}_{\vec{n}}$. To solve these equations we must determine $G^{\alpha}_{\vec{m}\vec{m}}, G^{\alpha}_{\vec{r}\vec{r}}$ as an explicit function of $\sigma_1^\alpha, \sigma_2^\alpha$ which is easily achieved by using Eq. (2.10).

Note that the SSA to obtain $\langle \mathcal{G}_{\vec{n}\vec{n}} \rangle^{A}_{\vec{n}}$ employs an effective medium characterized by σ_1^A, σ_2^A, while to approximate $\langle \hat{\mathcal{G}}_{\vec{n}\vec{m}} \rangle^{B}_{\vec{n}}$ it employs a different effective-medium characterized by σ_1^B, σ_2^B. The reference potentials σ_1^A, σ_2^A are energy dependent and are determined by solving Eqs. (2.28) simultaneously with $\alpha = A$. Likewise, the reference potentials σ_1^B, σ_2^B are also energy dependent and are obtained by solving Eqs. (2.28) simultaneously with $\alpha = B$. In both instances ($\alpha = A$ or B) these equations have several solutions which are a function of energy and the model parameters. The physical solution is always unambiguously chosen by asymptotic behavior as $|Z| = |E + is| \to \infty$ and then continued numerically using the techniques of the Appendix into the interesting range of eigenenergies within the band. In contrast to many other effective-medium theories,[7,8,14,16] no problems were encountered in employing this procedure even though in many instances δ was taken quite large ($\delta \sim 10$).

On the surface it may seem that inherent in the SSA is an obvious flaw that would in much of the parameter space seriously affect its ability to approximate accurately $\langle \mathcal{G}_{\vec{n}\vec{n}} \rangle^{\alpha}_{\vec{n}}$. Specifically, this method seems to make a crucial mistake in employing two sublattices; however, as we shall see, the errors incurred in this way, even when $P_{A/B}$ is considerably less than X_A are in fact small while the benefits gained when, for example, $X_A = 0.5, P_{A/B}$ close to 1 are large. Let us examine this question further. $\langle \mathcal{G}_{\vec{n}\vec{n}} \rangle^{\alpha}_{\vec{n}}$ depends on the environment within a mean free path or so of $\vec{n}$. Thus, when the mean free path is short, the SSA should be far superior to the CPA and even to the CSA, since it treats the environment of $\vec{n}$ more accurately than either of the latter two schemes. The fact that the SSA may incorrectly continue the $\sigma_1^\alpha, \sigma_2^\alpha$ arrangement all the way to infinity is immaterial in this case.

Another regime where the SSA obviously excels is the large $P_{A/B}$ regime when $X_A = 0.5$. In the 1D case the $\sigma_1^\alpha, \sigma_2^\alpha$ alternating arrangement is physically meaningful within a correlation length of the order of $-(\ln P_{A/B})^{-1}$ which is quite large as $P_{A/B} \to 1$. Moreover, in higher-dimensional lattices when $P_{A/B}$ exceeds a critical value P_c depending on the lattice [e.g., for the 2D square lattice ($P_c \approx 0.855$)] the $\sigma_1^\alpha, \sigma_2^\alpha$ two sublattice arrangement remains meaningful all the way to infinity, since when $P_{A/B} > P_c$, long-range order exists in the system which is created out of the AC. This can be easily seen by noting that correlating the A and B atoms through $P_{A/B}$ is exactly equivalent to an Ising coupling between spin up and down.[17] As a matter of fact the above value of $P_c \approx 0.855$ was obtained from Onsanger's solution of the two-dimensional Ising model.[17] Thus, in the regime of high $P_{A/B}$, SSA is very accurate, while both the CPA and the CSA fail there. Even the quite sophisticated cellular CPA (CCPA) developed by Butler,[8] although capable of incorporating partial ordering, is not accurate when $P_{A/B}$ is large; besides, we have found in this regime that the CCPA develops numerical difficulties when one tries to extrapolate the correct solution at high energies to the interesting range of energies within the band.

Also, as can be readily checked, the SSA like the CSA will reproduce the correct results for the total DOS to first order in the weak scattering limit, when the site diagonal energies are uncorrelated. Moreover, it is exact in all the nonrandom correlated limits of our model and gives the correct results in the atomic limit as well. Errors introduced by the use of two sublattices are most pronounced when $P_{A/B}$ is small (where the favored segregation of species cannot be effectively described by two interpenetrating sublattices) and for medium mean free path (not too short when the distant sites become immaterial; not too long when $\sigma_1^\alpha \approx \sigma_2^\alpha$). Even in this most unfavorable regime, we do not expect the whole spectrum to be affected equally. It is well known that the alternating $ABAB\ldots$ arrangements have severe effects around the center of the band, $E \approx (\epsilon^A + \epsilon^B)/V \equiv 0$, where a gap develops. Thus the SSA is expected to be at its worse for low $P_{A/B}$, medium mean free path, and E around zero. Our explicit results to be presented later support this analysis.

It should be stressed once more that the above comments about the properties of the SSA apply when this approximation is used to evaluate diagonal matrix elements $\langle \mathcal{G}_{\vec{n}\vec{n}} \rangle$ or other *local* quantities like $\langle \mathcal{G}_{\vec{n}\vec{m}} \rangle$, with $\vec{n}, \vec{m}$ nearest neighbors. The SSA would give very poor results if applied directly to the evaluation of $\langle \mathcal{G}_{\vec{n}\vec{r}} \rangle$ when $|\vec{n} - \vec{r}|$ is

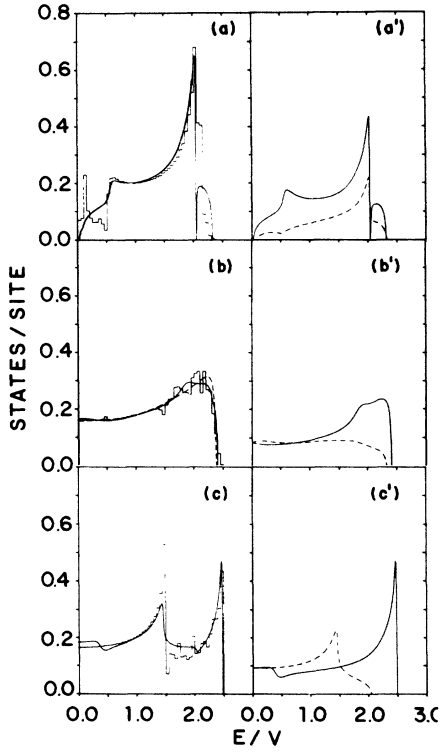

FIG. 3. Total electronic DOS per site [(a), (b), (c)] from the SSA (solid lines) and where appropriate, the CPA (dashed line) compared with the corresponding exact results (histogram) for a 1D alloy with $X_A = 0.5$, $\delta = 1$, and $P_{A/B}$: (a) 0.9; (b) 0.5; and (c) 0.1. Also shown [(a'), (b'), (c')] are the corresponding average state densities at an A atom $\rho^A(E)$ (solid lines), and a B atom $\rho^B(E)$ (dashed lines) from the SSA weighted by X_A and $X_B = 1 - X_A$, respectively. Note that $\rho^A(E) = \rho^B(-E)$, $\rho(E) = \rho(-E)$.

larger than the correlation length associated with $P_{A/B}$. To be on the safe side, the SSA (and the CSA for that matter) should be seen as approximation schemes for evaluating averages of *diagonal* matrix elements of $\langle \hat{g} \rangle$, or equivalently average DOS, and not averages of the total operator $\langle \hat{g} \rangle$.

To evaluate the effectiveness of the SSA as an interpolating approximation we have first applied it to the 1D random alloy; however, we stress that this scheme is also applicable with no additional approximations to any random alloys describable by our model. In presenting any new effective-medium approach such as the SSA, it is important to first test it in 1D since there exact results for the total DOS can be generated, for example, by solving Schmidt's functional equations. These exact results can be then compared to the corresponding approximate total DOS. Such detailed comparisons provide a severe test for any effective-medium technique since approximations of this type should improve with increasing dimensionality and as Elliott *et al.*[13] have noted it was just this sort of analysis that put the CPA on firmer ground.

To test the SSA and to see the effects of AC explicitly, we first display in Fig. 3 the total electronic density of states of a 1D alloy with $X_A = X_B = 0.5$, and $\delta = 1$, for three values of $P_{A/B}$, while in Figs. 4 and 5, we show how these results are changed as the relative scattering strength δ is increased to two and then to four where the bands are just split. For a given δ, the different values of $P_{A/B}$ are chosen to allow comparison involving the total DOS per site of the completely random alloy (here $P_{A/B} = 0.5$), the random alloy which has a tendency towards compound formation ($P_{A/B} = 0.9$) and the random alloy which has a tendency towards segregation of constituents ($P_{A/B} = 0.1$). These results show the severe effects that changing $P_{A/B}$ can have on the density of electronic states of our model when $X_A = 0.5$, and

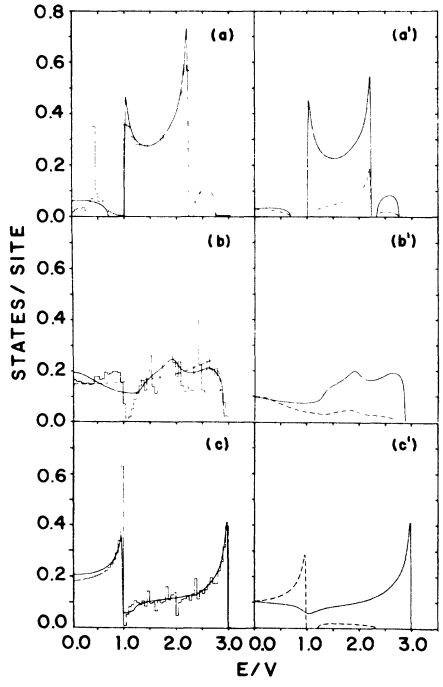

FIG. 4. Total electronic DOS per site [(a), (b), (c)] from the SSA (solid lines) and where appropriate, the CPA (dashed line) compared with the corresponding exact results (histogram) for a 1D alloy with $X_A = 0.5$, $\delta = 2$ and $P_{A/B}$: (a) 0.9; (b) 0.5; and (c) 0.1. Also shown [(a'), (b'), (c')] are the corresponding average state densities at an A atom $\rho^A(E)$ (solid lines), and a B atom $\rho^B(E)$ (dashed lines) from the SSA weighted by X_A and X_B, respectively. Note that $\rho^A(E) = \rho^B(-E)$, $\rho(E) = \rho(-E)$.

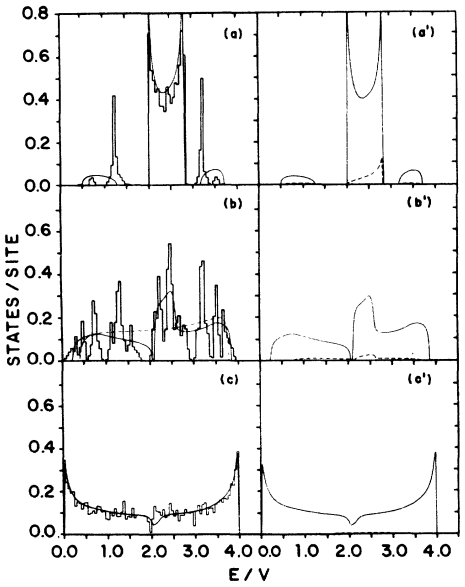

FIG. 5. Total electronic DOS per site [(a), (b), (c)] from the SSA (solid lines) and where appropriate, the CPA (dashed line) compared with the corresponding exact results (histogram) for 1D alloy with $X_A = 0.5$, $\delta = 4$ (just split band case) and for $P_{A/B}$: (a) 0.9; (b) 0.5; and (c) 0.1. Also shown [(a'), (b'), (c')] are the corresponding average-state densities at an A atom $\rho^A(E)$ (solid lines), and a B atom $\rho^B(E)$ (dashed lines) from the SSA weighted by X_A and X_B, respectively. Note that $\rho^A(E) = \rho^B(-E)$; $\rho(E) = \rho(-E)$.

thus emphasize the necessity of including statistical correlations amongst the atomic potentials in any analysis of the electronic structure of such alloys. For each $P_{A/B}$, the total DOS obtained by employing the SSA and, where appropriate, the CPA is compared to the exact results generated by solving the Schmidt's functional equations. In addition, in Figs. 3–5, we exhibit the average-state densities at an atom of type A, $\rho^A(E)$, and an atom of type B, $\rho^B(E)$, determined directly by the SSA and then used to obtain the SSA results for the total DOS, also shown in these figures. It should be noted that the SSA can be used to generate both the totally and partially averaged DOS at 250 points within the spectrum for less computational costs than required to solve Schmidt's functional equations accurately using Agacy's[18] techniques at just one point. Moreover, Schmidt's formalism is incapable of producing the conditionally averaged DOS shown in Figs. 3–5. These results taken all together indicate that the SSA is a surprisingly accurate scheme for uncovering many of the features of the exact DOS.

Although we do not display in this subsection any results showing the effects of AC when $X_A \neq 0.5$, we will do so in Sec. II E where it will be seen that as X_A is increased, the AC play a diminishing role, due to the increasing dominance of the majority constituent (here X_A) in determining the spectrum of states.

To analyze these results in further detail we first consider the "anticlustering" sequence shown in Figs. 3(c), 3(c')–5(c), 5(c'), where the alloy exhibits a fairly strong local tendency towards segregation of species ($P_{A/B} = 0.1$). By examining these figures, we see right away that the SSA is successful in reproducing quite accurately the exact results in this regime of small $P_{A/B}$. Although the SSA is doing a good job here, it is not doing as well as the CSA, as can be seen explicitly by comparing Figs. 3(c) and 2(c) and as could be expected from our previous analysis. The small differences in the approximate results from the SSA and CSA that can occur when $P_{A/B} < X_A$ are primarily due to the SSA's use of an effective medium different in form from the effective medium used by the CSA. As was noted before, the CSA's effective medium is more appropriate in this regime than that of the SSA's with the two sublattices. The fact [see Figs. 2(c) and 3(c)] that the differences in the approximate results from the SSA and the CSA are most pronounced around $E = 0$ when $P_{A/B} = 0.1$, $X_A = 0.5$ and $\delta = 1$, is in agreement with our previous conclusions. Since this particular problem with the SSA is of a global nature (i.e., associated with its effective medium), it is not quite rectified by the cluster extensions that we present in Sec. II E. We have called attention to this very slight difficulty to emphasize how little error is really introduced in this approximation by the use of two distinct sublattices even when $P_{A/B} < X_A$. Since it is just this feature that allows the SSA as opposed to the CSA to interpolate successfully into the parameter region where $P_{A/B} > X_A$, and to reproduce the periodic compound formation limit $X_A \to 0.5$, $P_{A/B} \to 1$, it is a very small sacrifice to make in order to obtain a much more generally applicable scheme.

The most prominent feature of all the results when $P_{A/B} = 0.1$ is their similarity to what would be obtained at the limit $P_{A/B} = 0$. In particular, as shown in Figs. 3(c'), 4(c'), and 5(c'), the average state density localized around an A atom is quite like the total DOS per site for the perfect A crystal while the average state density localized around a B atom is similar to the total DOS per site of the perfect B crystal. It is somewhat surprising that the very sharp band edges associated with either the perfect A or B crystal are not more rounded by the introduction of the non-negligible randomness $P_{A/B} = 0.1$. We also see from these figures that as the scattering strength is increased the

average state density localized around an atom of type α becomes progressively more associated with states of parentage α, where the parentage is clearly registered in the atomic limit. Finally, to conclude our discussion of the segregated regime we note that the SSA splits the band right around $\delta = 4$, a result which is in agreement with the exact critical value of δ necessary for splitting predicted from the Saxon-Hunter[19] localization theorem.

Now consider the random sequence ($P_{A/B} = X_A = 0.5$) shown in Figs. 3(b)–5(b′) and 6. We first note that when the difference between the two constituents is not large ($\delta = 1$), both the CPA and the SSA yield approximate densities of states that are in good agreement with the exact results. This is not at all surprising since both schemes are exact in the virtual crystal limit ($\delta \to 0$) and thus are expected to do well when δ is small. However, as the relative scattering strength is increased [check Figs. 4(b) and 5(b)] both approximations become progressively less successful. We see though as $|\delta|$ increases, the results from the SSA are all and all progressively more satisfactory than those from the CPA. This is to be expected since the SSA like the CSA stresses in its self-consistency conditions the partial inclusion of local effects on the conditionally averaged DOS, while the CPA ignores them completely and these effects are of course increasing in importance as the states acquire a shorter mean free path with increasing $|\delta|$. If this explanation is in fact correct, then the SSA in this regime should also be superior to the CSA, since its approximate results are more aware of the environment around $\vec{n}$. In all cases where we have tested this conjecture, we have found it true and a particular example is shown in Fig. 6, where it is shown that the SSA on the whole shifts the states less severely from their correct values.

As with the segregated sequence, we see also with this uncorrelated sequence that as the difference between the atomic levels is increased, the band is split into two subbands, with each being made up almost entirely of states associated with a particular type of atom. When $X_A = P_{A/B}$, the SSA splits the bands less readily than the CPA, but still too easily.

Although the SSA is not producing the fine structure of the band in Fig. 6, it is really shifting states only locally from their correct values as is shown explicitly in Fig. 6(a), where the cumulative total DOS from the SSA is compared to the exact results from Schmidt's functional equations. This point is important since it means that although these results from the SSA cannot be used to analyze the fine detail of the band there, they should be perfectly adequate for thermodynamic calculations when the temperature is not too low.

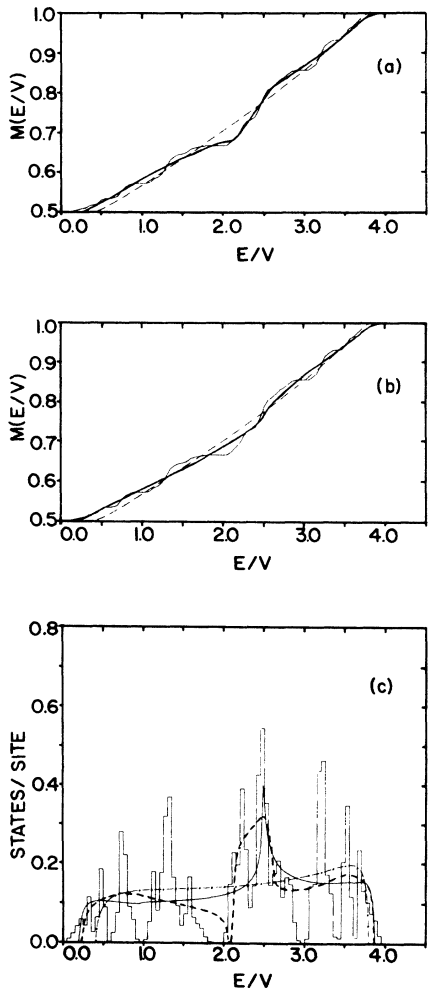

FIG. 6. (a) Cumulative DOS from the SSA (thick solid line), CPA (dashed line), and Schmidt's equations (thin solid line); (b) Cumulative DOS from the CSA (thick solid line), CPA (dashed line), and Schmidt's equation (thin solid line); (c) Total DOS from the CPA (dashed dotted line), CSA (solid line), SSA (dashed line) and Schmidt's equation (histogram); $\delta = 4$, $P_{A/B} = X_A = 0.5$.

We now turn our attention to the sequence exhibiting a tendency towards local compound formation, Figs. 3(a)–5(a′). It is evident from these results that the SSA has the ability to interpolate into the region $P_{A/B} \gtrless X_A$, and produces well in all cases the residue of the periodic limit ($X_A = 0.5, P_{A/B} = 1$) found in the exact results. Although this method is having problems with the two prominent impurity "bands" that are shown in each figure, it qualitatively reproduces their behavior as the relative scattering strength is increased. These impurity bands result from states localized around points where large periodic AB

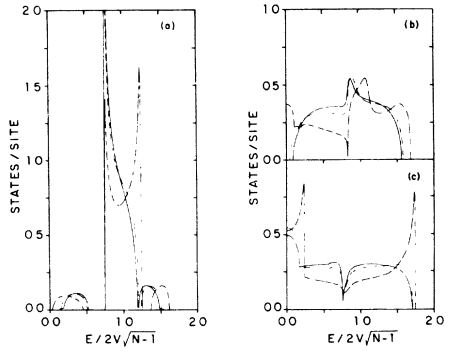

FIG. 7. Total DOS of a binary Cayley-tree alloy from the SSA for $P_{A/B}$: (a) 0.9; (b) 0.5; and (c) 0.1, and coordination number N: 2 (dashed dotted line); 4 (dashed line); and 6 (solid line); $\delta/4(N-1)^{1/2}=0.75$, and $X_A=0.5$. All curves are symmetric around $E=0$.

clusters have been improperly connected. They are not associated with the replacement, for example, of an A atom at some site in the periodic AB compound by a B atom. As with the segregated and totally random sequences, we see that as the relative scattering strength is increased, states of parentage A are increasingly depleted from the allowed region of eigenvalues around ϵ^B and vice versa.

The most interesting feature of these results is, of course, their similarity to the totally periodic case, $X_A=0.5, P_{A/B}=1$, even though the atomic correlation is not that strong ($P_{A/B}=0.9$). This happens in higher dimensions as well, and thus, when dealing with random alloys thought to have a local tendency toward periodic compound formation, one should be alert to the possibility of a rather drastic depletion of states in the center of the band. Moreover, in this picture,[20] the states remaining in the gap should be strongly localized so that most probably in higher dimensions one is left with a semiconductorlike DOS with localized states inside a gap that separates the valence from the conducting band.

In Fig. 7, we show the effects of AC on the total DOS of several alloys having equal constituent concentrations and Cayley-tree lattice structures of coordination numbers two (1D), four, and six, where the latter two cases effectively represent higher-dimensional systems. These results were obtained by applying the SSA, and the different values of $P_{A/B}$ were taken as 0.1, 0.5, and 0.9. In each instance, the energy is normalized by $1/(N-1)^{1/2}$ and the relative scattering strength taken so that $\delta/4(N-1)^{1/2}=0.75$, where here N represents the lattice coordination number. This was done to emphasize that under these circumstances after N becomes larger than two the Cayley-tree DOS differs little in form as the coordination number is changed. This fact has nothing at all to do with the SSA as can be seen by examining the analytic form of the DOS in any of the periodic limits. It is simply a feature of Cayley trees that has gone largely unrecognized in the literature. Further, note that when the coordination number is infinite, the crystalline Cayley-tree Green's function simply becomes the Hubbard or semicircular Green's function if $\delta/(N-1)^{1/2}$ is kept constant as N is increased. This Cayley lattice with infinite coordination number has been used extensively by Velicky *et al.*[15] to study the simple CPA. Moreover, the DOS in this case does not differ much from what is obtained by taking $N=4$, 6, etc.

We see from Fig. 7 that when $X_A=X_B$, AC has effects on the band structure of random Cayley alloys with coordination numbers other than two qualitatively identical to those found in the 1D case. Explicitly, a tendency toward local periodic compound formation results in much fewer states around the center of the band than would be found, for example, in the purely random and segregated regimes.

The evident success of the SSA in handling our model for arbitrary $P_{A/B}$ in 1D strongly indicates that it will be an even more successful approximation scheme in higher-dimensional systems where exact procedures are absent. This follows since this approach has been found to have its greatest difficulties in 1D around energies where the actual spectrum of the system exhibits very sharp peaks and although such structure in the DOS exists in higher dimensions, it is of decreasing importance. Thus, we expect our model in conjunction with the SSA to be very helpful in analyzing both quantitatively and qualitatively the effects on the electronic structure of random alloys in the presence of short-range statistical correlations amongst the atomic potentials in real systems.

E. Generalizations of the SSA

All of the approximation schemes that we have introduced up to this point use only the simplest possible random hybrid Green's function. Although our best scheme so far, the SSA, is very successful in incorporating many of the effects of short-range order, it does not uncover the very fine structure that is expected in the density of states when the electron's mean free path is short. Thus it cannot, for example, be used to analyze the erratic structure that occurs in the 1D band when the relative scattering strength δ is fairly strong, the system is completely random, and the concentration of both constituents is large (check

Fig. 6). Moreover, it does not reproduce a completely satisfactory DOS at eigenenergies associated with impurity states. These problems essentially arise because the SSA fails to incorporate into its effective Green's function enough of the effects of the environment around the site where the conditionally averaged DOS is calculated and are expected to be partially alleviated by an approximation scheme employing a larger cluster $\tilde{c}$. To develop such an approach is straightforward in one dimension (or, for that matter, whenever a Bethe lattice is assumed) but as we shall see, more difficult in higher dimensions because of symmetry problems associated with self-consistently defining the effective medium. The cluster approximation that we present below in the framework of the 1D lattice will be termed the cluster-SSA(CSSA) and, for example, it is able to reproduce (at considerably less cost) all the many very sharp peaks that are shown in the histogram of Fig. 6. Although this method is applicable in principle to any random binary Cayley-tree system treatable by our model, it unfortunately, unlike the SSA, cannot be carried over directly to real two- and three-dimensional lattices. It can, however, as we shall discuss at the end of this subsection, be used as a basis for a tractable cluster approximation applicable in higher dimensions, and as such is a technique of considerable interest.

As noted above, to incorporate into the totally and conditionally averaged DOS more of the effects associated with the local environment around the site $\vec{n}$, we should begin with a more complicated hybrid random Green's function than used by the SSA. In particular, in the CSSA, which we present now, we start with a random hybrid Green's function, $\hat{G}^c$, where $\tilde{c}$, is a cluster *centered* around $\vec{n}$. By following reasoning processes analogous to those which led us to the SSA, we find that the effective medium to be used by $\hat{G}^c$ in approximating $\langle \hat{\mathcal{G}}_{\vec{n}\vec{n}} \rangle_{\tilde{c}}^c$ should be characterized by four coherent potentials $\sigma_i^c; i = 1,4$. These potentials are arranged on the chain in such a manner that to the right of the fixed cluster we have σ_1^c, σ_3^c at alternating sites, while to the left we have σ_2^c, σ_4^c at alternating sites (check Fig. 8); all four of these coherent potentials are determined self-consistently by requiring, in the spirit of the CSA and SSA, that the average scattering matrices associated with the nearest- and next-nearest neighboring sites to the cluster of fixed configuration $\tilde{c}$ be zero. With these specifications, the CSSA is defined and can be summarized as taking each

$$\langle \mathcal{G}_{\vec{n}\vec{n}} \rangle_{\tilde{c}}^c \approx G_{\vec{n}\vec{n}}^{\tilde{c}} = \langle (\vec{n} | (\hat{Z} - \hat{H}^c)^{-1} | \vec{n}) \rangle_{\tilde{c}}^c , \tag{2.29}$$

where the quantities $\sigma_i^c, i = 1, 4$, which together with the cluster $\tilde{c}$ define $\hat{H}^c$, are determined from the four self-consistent conditions

$$\langle \hat{t}_{\vec{n}_{k+i}}^c \rangle_{\tilde{c}}^c = 0 ; \quad i = 1, 4 . \tag{2.30}$$

(k is the number of sites contained in $\tilde{c}$.) This way of self-consistently determining $\hat{G}^c$ will yield the exact results in any of the coherent-model limits. Also when the number of sites contained in $\tilde{c}$ is one, the CSSA immediately collapses into the SSA since in this instance $\sigma_1^c = \sigma_2^c, \sigma_3^c = \sigma_4^c$ and there are only two configurations: A, B.

For the purpose of numerical calculations, the self-consistent conditions for $\sigma_i^c, i = 1, 4$, can be recast as

$$\bar{\epsilon}_i^c - \sigma_i^c - (\epsilon^B - \sigma_i^c) G_{\vec{n}_{k+i}\vec{n}_{k+i}}^c (\epsilon^A - \sigma_i^c) = 0 ; \quad i = 1, 4 , \tag{2.31}$$

where $\bar{\epsilon}_i^c \equiv \langle \epsilon_{\vec{n}_{k+i}} \rangle_{\tilde{c}}^c$ (check Fig. 8). Although Eq. (2.10) could be used to obtain the desired matrix elements of $\hat{G}^c$ as an explicit function of $\sigma_i^c, i = 1, 4$, it is simpler since we only need diagonal matrix elements of this operator to use the renormalized perturbation expression[21] which allows these quantities to be written elegantly as continued fractions in terms of $\sigma_i^c, i = 1, 4$. Thus the CSSA approximates each $\langle \hat{\mathcal{G}}_{\vec{n}\vec{n}} \rangle_{\tilde{c}}^c$ separately (for a cluster composed of k sites, there are 2^k of these corresponding to the 2^k different arrangements of the A, B atoms over the cluster), by employing an effective medium characterized by four coherent potentials $\sigma_i^c, i = 1, 4$, which are dependent and are determined solely by solving the four equations (2.31) simultaneously. As with the SSA's self-consistent conditions, the physical solution to Eqs. (2.31) are chosen by their asymptotic behavior at infinity and then continued numerically using the techniques of the Appendix to the interesting range of energies within the band. Once again, no problems were encountered in employing this procedure. Finally, having approxi-

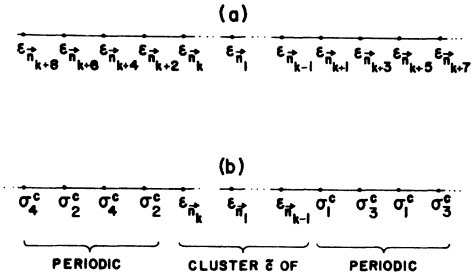

FIG. 8. Schematic outline of the CSSA which in approximating $\langle \mathcal{G}_{\vec{n}\vec{n}} \rangle_{\tilde{c}}^c$ replaces the actual random medium (a) by the random hybrid medium (b) and determines the free parameters σ_i^c ($i = 1, 4$) by requiring that the average of the random scattering matrices $\langle \hat{t}_{\vec{n}_{k+i}}^{\tilde{c}} \rangle_{\tilde{c}}^c$ $i = 1, 4$ equal zero.

mated through the CSSA each $\langle \mathcal{G}_{\vec{n}\vec{n}} \rangle_{\tilde{c}}^{c}$ separately, total or partial DOS can be easily obtained.

To understand how much numerical work is necessary to generate in this manner the totally and conditionally averaged DOS, suppose $\tilde{c}$ is composed of k sites. Then there are 2^k possible arrangements (configurations) of the A, B atoms over this cluster, so we must determine $2^k \times 4$ coherent potentials self-consistently. This is easier than may be thought since: first, we do not have to determine all of these quantities simultaneously, but, at worst, in groups of 4; secondly, we only have to treat half of the asymmetric configurations since for each of these there is another which is its mirror image around $\vec{n}$ and in the CSSA both of these configurations contribute equally to the approximate totally and conditionally averaged DOS; finally, if a particular configuration is symmetric about $\vec{n}$, then $\sigma_1^c = \sigma_2^c$ and $\sigma_3^c = \sigma_4^c$ as can be easily seen from Eqs. (2.31) so rather than solving four equations simultaneously to determine $\sigma_i^c, i = 1, 4$, we need for this case to solve only two. In terms of cost, the five-site CSSA can be used to generate the conditionally and totally averaged DOS for a little less than one-third the cost required to generate similar results by solving Schmidt's functional equations using the techniques of Agacy.[18] It is important to note also that not only does the CSSA produce for this cost the totally and conditionally averaged density of states but simultaneously generates the 2^k conditionally averaged state densities $\rho^c(E)$ each of which gives the average-state density localized around a particular configuration of atoms over the five-site cell. These quantities of course give a lot of information that can be used most informatively to analyze the total spectrum.

In Fig. 9(a)–9(c), we show the evolution of the total DOS from this approximation for an alloy with $X_A = 0.75, P_{A/B} = 0.6, \delta = -3.2$ as the number of sites k in the cluster is increased from one to three and finally to five. When k is as small as three, most of the features of the corresponding histogram have been revealed and at five, the agreement between the two results is really astonishing. The very sharp peaks in the impurity region of the spectrum ($E/V > 0.4$) are associated with states localized on B-rich clusters which are surrounded locally by pure chains of A atoms.[22] This is easy to see since in this region of E/V, the pure A chain has no propagating solutions and as a result, the A atoms surrounding a B-rich cluster have a tendency to localize the wave functions associated with that cluster. In this light, for example, the most prominent peak in this impurity region is expected to be associated with single B atoms isolated in an A environment, and this is

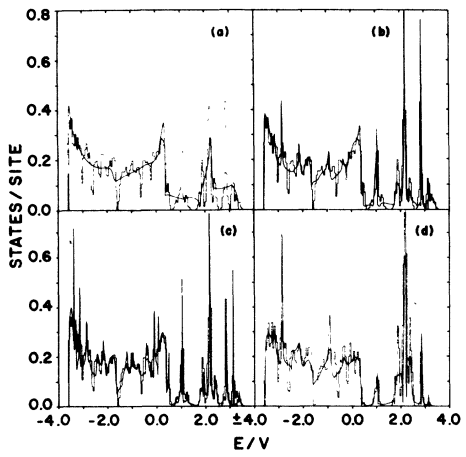

FIG. 9. Exact total DOS (histogram) for a 1D alloy with $X_A = 0.75$, $P_{A/B} = 0.6$, and $\delta = -3.2$ compared to the corresponding results from the CSSA as the number of sites in the cluster $\tilde{c}$ is increased from one (a) to three (b) and then to five (c). Also shown (d) is the total DOS (histogram) for a 1D alloy with the same X_A, δ as in (a), (b), and (c) but with $P_{A/B} = 0.9$ compared to the corresponding results from the three-site CSSA.

exactly what is found. The less prominent peaks that appear in the region of the spectrum allowed to both the pure A and B crystals cannot have the same origin as those in the impurity band and the interested reader is referred to the work of Papatriantafillou[23] for an analysis of structure of this type. The effects in this example of increasing $P_{A/B}$ from 0.6 into the region of local random compound formation ($P_{A/B} = 0.9$) is shown in Fig. 9(d). We see here that the CSSA is also performing admirably, but the point that we want to make with this example is the diminishing importance of statistical correlation amongst the atomic potentials when X_A is different from 0.5. This of course results because of the increasing dominance in the spectrum of states associated with the majority constituent. Thus, when X_A is appreciably different from 0.5, and the atomic correlation is not too strong, in many instances it should not be such a bad approximation to simply consider the system as though $P_{A/B} = X_A$. However, if the atomic correlation is very strong, particularly in the anti-clustering regime, the effects of statistically correlating the atomic potentials can still be important, as one can see trivially from our discussion of the limit $P_{A/B} \to 0, X_A$ arbitrary, in Sec. IIC.

In Fig. 10, we compare the total DOS from the three-site CSSA and CCPA to the corresponding exact results. As could be expected from our comparisons of the CPA to the SSA, results from the three-site CSSA are better than those from the three-site CCPA, although both methods are work-

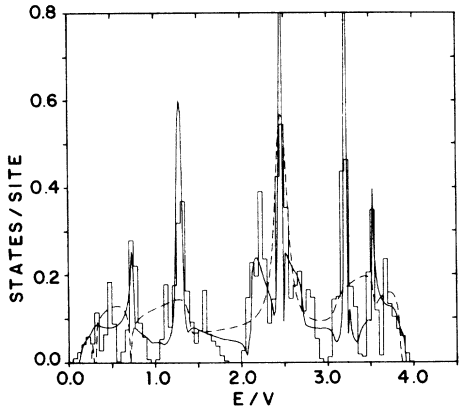

FIG. 10. Total DOS from the three-site CCPA (dashed line) and CSSA (solid line) compared to the exact results (histogram) for the 1D alloy with a just split band ($\delta = 4$) and $X_A = P_{A/B} = 0.5$. All curves are symmetric about $E = 0$.

ing well. The same is true for larger clusters. Away from the uncorrelated case $X_A = P_{A/B}$, whenever one has need for such approximations, the CSSA will improve significantly its superiority over the CCPA since, for example, the latter scheme cannot reproduce the periodic compound formation limit ($X_A = 0.5, P_{A/B} = 1$). Finally, in Fig. 11 for the sake of comparison we present the totally and conditionally averaged DOS from the five-site CSSA for a case studied earlier in discussing the SSA. As can be seen by examining this figure the five-site CSSA consistently reproduces correctly almost all the features of the histograms.

Although the CSSA in light of the above results is clearly a completely satisfactory cluster approach in 1D and can be simply generalized to treat any Bethe lattice, it, unlike the SSA, is not directly applicable to higher-dimensional systems. To understand the problem, it is simplest to explain in some detail our reasons for using four coherent potentials as opposed to two in formulating the CSSA. The reader may have wondered when we introduced the CSSA why we did not in fact employ only two coherent potentials arranged over the chain in just the same way as in the SSA, since after all in that instance by simply setting the average scattering equal to zero at a nearest neighboring and next-nearest neighboring site at one edge of the fixed cluster, we would reproduce all the coherent limits of the model. Doing this however is undesirable since this approach, which we will term the CSSA-2, treats configurations of atoms asymmetric about the center of the cluster $\tilde{c}$ not as well as the CSSA, while being essentially no less expensive computationally. More specifically, due to the asymmetry of the configurations and the local nature of the self-consistent equations, we would now no longer as we really should, obtain identical contributions to the total DOS from this cluster and its mirror image. To get around this problem in 1D, we used four coherent potentials and similar games can always be played with any Bethe lattice; however, for real two- and three-dimensional lattice structures, such a generalization of the SSA is clearly not obtainable. So if we are to produce a cluster approximation applicable to higher-dimensional systems while still staying in the mainstream of our present development, we are essentially stuck with the CSSA-2. However, we note that the real reason for generalizing the SSA at all is to resolve in the DOS some of the very fine structures that may exist there and this structure is usually associated with states very localized in real space. Under these circumstances, we then expect in many instances that the CSSA-2 will work very nicely, and so propose it as a useful scheme for uncovering

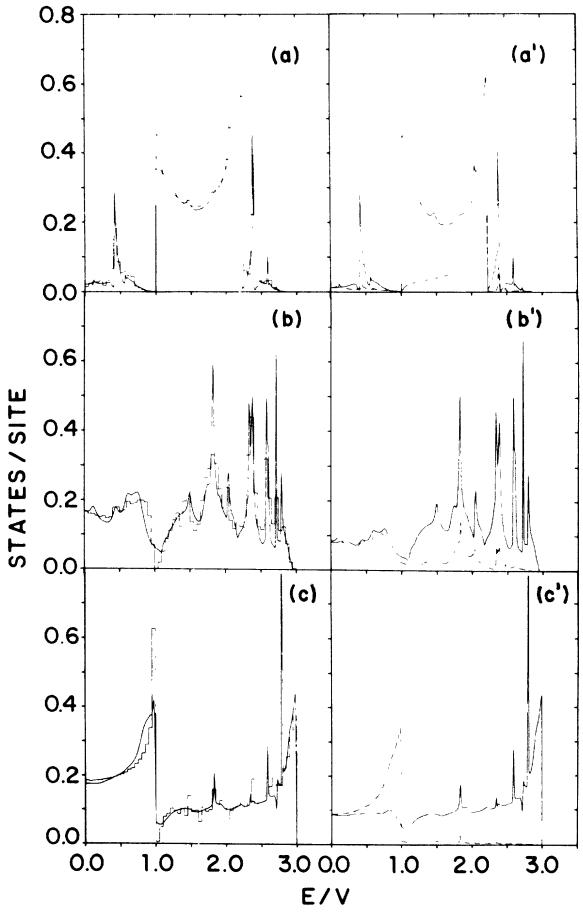

FIG. 11. Results from the five-site CSSA (solid line) and exact results (histogram); parameters as in Fig. 4.

many of the features missed by the SSA.

In closing this section, we note that our cluster methods are directly applicable to models exhibiting long-range as well as short-range ordering of the atomic potentials, and this should be kept in mind when investigating the electronic structure of such systems.

III. CONCLUSIONS

We have studied the popular two-level tight-binding model of a substitutionally disordered binary ($A_{X_A}B_{X_B}$) alloy including the possibility of statistical correlations amongst the atomic potentials. Results from this study show the severe effects AC can have on the electronic structure of alloys (particularly those for which $X_A = 0.5$), and thus emphasize that one should be alert to the possibility of such effects in any analysis of systems of this type.

In the framework of this model we have developed two new self-consistent effective-medium theories (CSA, SSA) that allow easy approximate determination of the totally and conditionally averaged DOS of alloys having a strong tendency towards local compound formation all the way to those having a strong tendency towards local segregation of species. To evaluate the effectiveness of these schemes, we have applied them to the 1D alloy since in this instance the approximate results can be compared to the corresponding exact results. Here we found that these methods are surprisingly successful and since they should improve with increasing dimensionality we expect them to work well in higher dimensions where exact procedures are absent.

In addition, in the context of 1D we generalized the SSA to an n-site cluster approximation (the CSSA) that was able to reproduce accurately the very fine structure known to exist there in the eigenvalue spectrum. The CSSA is the first such effective-medium theory that has this capability in the presence of AC. This cluster approximation is applicable to Cayley trees of coordination numbers other than two as well, and when coupled with the additional approximations discussed at the end of Section II E, will be a very useful tool for studying higher-dimensional systems.

Finally, we have built a conceptual framework that can be employed to develop self-consistent effective-medium approximations for obtaining the totally and conditionally averaged densities of states in random tight-binding models assuming for example, long-range as well as short-range ordering of the atomic potentials, off-diagonal randomness, or continuous as opposed to discreet probability distributions of the random variables.

ACKNOWLEDGMENT

One of us, C.T.W., would like to thank Dr. C. T. Papatriantafillou for several stimulating discussions involving this work.

APPENDIX: NUMERICAL METHODS FOR SOLVING THE SELF-CONSISTENT EQUATIONS OF THE CSA, SSA, AND CSSA

To apply any of the approximation schemes that we have presented in this work we must be able to solve either singly, as with the CSA, or simultaneously, as with the SSA and CSSA, a small number of highly nonlinear equations which implicitly and self-consistently complete the definitions of the effective Green's functions which we use when approximating the quantities of interest. To do this we have developed a somewhat complicated but highly efficient numerical technique based on the Newton-Raphson procedure. The salient features of this technique are most easily outlined by sketching how we solve the single self-consistent Eq. (2.16) of the CSA that defines the single effective potential σ^α which is a complex function of the energy, concentration, scattering strength, and the AC parameter.

Equation (2.16) defines implicitly several branches of the complex function $\sigma^\alpha(Z)$; however, the correct one must be such that $\lim_{Z\to\infty}\sigma^\alpha(Z) = \langle \epsilon_{\vec{m}} \rangle_{\vec{n}}^{\alpha}$. Since the quantity of interest $\rho^\alpha(E)$ is given by (2.4), we need to determine $\sigma^\alpha(E+i0^+)$ only. This we achieve by using the Newton-Raphson method to first obtain $\sigma^\alpha(E+i\eta)$ with $\eta = 0.05$, at each point of interest E and then (again using the Newton-Raphson procedure) we take the limit $\eta \to 0^+$ numerically. One may wonder why not follow the simpler path $f(Z) = E + i0^+$, and thus obtain $\sigma^\alpha(E+is)$ directly. However, this is in fact more difficult numerically since there are problem points encountered along this line which one cannot get through easily. These are not branch points, but points essentially centered in an interval along $f(Z)$ where the left-hand side of (2.16) changes so rapidly with respect to σ^α that it is no longer feasible to apply the Newton-Raphson technique.

To solve the SSA's two self-consistent equations for $\sigma_1^\alpha(E)$, $\sigma_2^\alpha(E)$ and thus obtain $\rho^\alpha(E)$ we simply use the 2D version of the above method, while to solve the CSSA's four self-consistent equations for $\{\sigma_i^c(E); i = 1, 4\}$, and thus obtain $\rho^c(E)$, we employ the 4D version.

*Work supported in part by NSF: Grant No. DMR 72-03279-A01.

†Present address: Naval Research Laboratory, Washington, D.C. 20375.

[1]D. W. Taylor, Phys. Rev. 156, 1017 (1967).
[2]P. Soven, Phys. Rev. 156, 809 (1967).
[3]J. Hubbard, Proc. R. Soc. Lond. A 281, 401 (1964).
[4]M. Lax, Rev. Mod. Phys. 23, 287 (1951).
[5]K. F. Freed and M. H. Cohen, Phys. Rev. B 3, 3400 (1971).
[6]L. Schwartz and E. Siggia, Phys. Rev. B 5, 383 (1972).
[7]V. Čapek, Phys. Status Solidi B 52, 399 (1972).
[8]W. H. Butler, Phys. Rev. B 8, 4499 (1973).
[9]See, e.g., H. Shiba, Prog. Theor. Phys. 46, 77 (1971); E-Ni Foo, H. Amar, and M. Ausloos, Phys. Rev. B 4, 3550 (1971).
[10]H. Schmidt, Phys. Rev. 105, 425 (1957).
[11]E. N. Economou and C. T. White, Phys. Rev. Lett. 38, 289 (1977).
[12]D. C. Licciardello and E. N. Economou, Solid State Commun. 12, 1275 (1973).
[13]R. J. Elliott, J. A. Krumhansl, and P. L. Leath, Rev. Mod. Phys. 46, 465 (1974).
[14]W. H. Butler and B. G. Nickel, Phys. Rev. Lett. 30, 373 (1973).
[15]B. Velický, S. Kirkpatrick, and H. Ehrenreich, Phys. Rev. 175, 747 (1968).
[16]W. H. Butler, Phys. Lett. A 34, 203 (1972).
[17]K. Huang, *Statistical Mechanics* (Wiley, New York, 1963), Chaps. 16 and 17.
[18]R. L. Agacy, Proc. Phys. Soc. Lond. 83, 591 (1964).
[19]See, e.g., D. J. Thouless, J. Phys. C 3, 1559 (1970).
[20]M. H. Cohen and J. Sak, J. Non-Cryst. Solids 8, 696 (1972).
[21]See, e.g., P. W. Anderson, Phys. Rev. 109, 1492 (1958); E. N. Economou and Morrel H. Cohen, Phys. Rev. B 4, 396 (1971).
[22]P. Dean, Proc. R. Soc. A 260, 263 (1961).
[23]C. T. Papatriantafillou, Phys. Rev. B 7, 5386 (1973).